ISSN : 0974 - 7443 Volume 7 Issue 3
CHEMICAL TECHNOLOGY
An Indian Journal
Full Paper
Trade Science Inc.
CTAIJ 7(3) 2012 [67-78]

Transalkylation and disproportionation of 1,2,4 trimethylbenzene over faujasite zeolite

S.A.Hanafi[1], M.S.Mohamed[1]*, A.A.Elkahlawy[1], S.A.Abo-El-Enein[2]
[1]Egyptian Petroleum Research Institute, Nasr City 11727, Cairo, (EGYPT)
[2]Department of Chemistry, Faculty of Science, Ain-Shams University, Cairo, (EGYPT)
E-mail : elmelawy@yahoo.com

ABSTRACT

Large pore faujasite zeolite (Pt/H-Y) and its dealuminated form (Pt/H-DY) were applied for transalkylation of toluene and 1,2,4-trimethylbenzene (1,2,4-TMB). The acidic properties of supports were examined by using NH_3-TPD and FT-IR spectroscopy in the OH stretching region. XRD, SEM, DSC and FT-IR in the framework region techniques were employed to investigate the structural changes of zeolite after dealumination process. It was observed that the dealuminated catalyst tends to have more open structure; such structural changes are believed to compensate for the loss of some acid sites to bring about the enhanced activity and stability over the parent zeolite. The zeolite structure has a direct influence on aromatics conversion. It was found that the use of 1,2,4-trimethylbenzene (TMB) as an alkylation agent gave the highest yield of xylenes. A strong competition between transalkylation, disproportionation and isomerization of aromatic hydrocarbons takes place according catalyst acidity and reaction temperature.

INTRODUCTION

As it is well known, that xylenes (Xs) are important starting materials for the industrial processes like the production of synthetic fibers, plasticizers and resins. The major sources of these aromatic hydrocarbons, the reforming and pyrolysis gasolines, have also an appreciable content of toluene (T = C_7) and trimethylbezenes. (TMBs = C_9). A convenient way to upgrade low value C_7 and C_9 aromatics consists of their conversion to benzene (B) and xylene (X). In this context, various processes such as: the disproportionations of toluene and trimethylbenzenes, the toluene alkylation with methanol, the toluene and alkylbenzenes hydrode-alkylation or the toluene and trimethylbenzenes transalklyation have been developed[1-3].

The term transalkylation generally refers to the reaction of polyalkylated aromatics by transfer of alkyl groups and formation of lower alkylated aromatics. For instance, by this method, some of the lo w valued by – products such as polyethyl and polyisopropyl benzenes are converted to their mono-substituted homologues having higher demands[5]. The transalkylation of toluene with TMBs forming xylenes is also an important process in this field. Acid catalysts activate this last equilibrium reaction. The commercial T–TMBs transalkylation processes use either silica – alumina or zeolite – based catalysts, e.g., noble metal supported on dealuminated mordenite[6].

Because of the large molecule aromatic hydrocarbons involved in the transalkylation reaction, only molecular sieves with large pore such as beta, faujasite-Y and SAPO-5[7] are able to catalyze this reaction. From the above literature survey, the pore size and the acidity of zeolites may be the two factors of a good catalyst for transalkylation[8]. First, only zeolites with 12-membered ring-opening possess a pore size large enough for transalkylation of C_9^+ aromatics. Second, the higher

acidity of the zeolities, the better is the activity.

In the present study, we investigated the catalytic activities of Pt supported on H-Y zeolite which has 12-MR pore openings, and of its dealuminated form. We also examined the physicochemical properties of the supports and the catalysts by various characterization techniques and the effects of dealumination on the activity and stability of zeolite for transalkylation of toluene and 1,2,4-trimethylbenzene (1,2,4-TMB). In commercial processes such as BTX units, TMB isomers are the major components in C_9 aromatics and the fraction of 1,2,4-TMB among three isomers is about 65%[9]. For this reason, toluene and 1,2,4-TMB were used as the reactants.

EXPERIMENTAL

Support preparation

Commercial NaY (SK-40) provided by union carbide Co., USA, was used for catalysts preparation.

NH_4-Y was prepared by exchange the sodium ion in Na-Y zeolite several times with ammonium nitrate (NH_4NO_3) molar solution; each time with a fresh solution for 8h at 70°C. The zeolite was then separated, washed with bidistilled water till free of the NO_3^+, and then dried at 110°C overnight.

NH_4-Dealuminated sample (NH_4-DY) was prepared by extraction of some aluminum oxide from NH_4-Y by refluxing 20gm sample in 300cm^3 doubly distilled water with 9.6gm of $(NH_4)_2H_2$ EDTA for 4h. The treated sample was then separated, washed and dried as mentioned above. Details on the dealumination procedure are given in earlier studies[10].

H-Y and H-DY samples were prepared by calcination of the NH_4-Y and NH_4-DY at 450°C for 4h. This temperature was chosen for pretreatment as at 450°C thermal dealumination doesn't occur in any case and a complete deammoniation can be achieved[11].

Catalyst preparation

The required quantity of hexachloroplatinic acid ($H_2PtCl_6.x\,H_2O$), necessary for loading 0.5wt% Pt, was dissolved in bidistilled water sufficient to cover the support material in a beaker. A small quantity of citric acid was added to enhance penetration of the precursor molecules from the solution into the pores of the catalytic support[11,12]. This preparation was left overnight at room temperature then dried at 110°C overnight. The catalyst was calcined in air for 4h at 450°C and reduced at 400°C in H_2 flow of 20cm^3 min^{-1} in a flow reactor for 2 h[13]. The physicochemical properties of the two catalysts are summarized in TABLE 1.

TABLE 1 : Physicochemical properties of the supports

Support	SiO_2/Al_2O_3	Na_2O	Textural properties		
			BET surface area, m^2/g	Pore volume, cc/g	Average pore diameter[a], Å
H-Y[b]	2.7	0.11	624	0.27	17.3
H-DY[c]	7.0	0.01	540	0.35	26

a: Average pore diameter = $\frac{4(\text{pore volume})}{\text{surface area}}$, b: H-Y support, and c: Dealuminated Y support

Support and catalyst characterization

Elemental analysis was performed by X-ray fluorescence (XRF) method. Surface area and pore volumes of the supports were determined by measuring the nitrogen adsorption-desorption isoltherms at 77K (BET method) using Micromeritics Gimini 2375 surface area analyzer, while porosity was determined by poresizer 9320-V2-08. The measurements were performed on samples heated at 200°C for 2 h in a pure nitrogen flow. Since the average pore sizes of these samples are small, the mercury penetration method was inadequate in the present study.

Infrared (IR) spectra were recorded on a ATI Mattson Infinity series Apparatus, Model 960 M0009, for characterization of supports and catalysts. The final spectra were taken after 64 scans with 2 cm^{-1} resolution.

Temperature-programmed desorption of ammonia (NH_3-TPD) was used to characterize the acid property of the used samples[14]. X-ray powder diffraction (XRD) patterns have been recorded on a Brucker AXS-D8 Advance (Germany) by using nickel-filtered copper radiation (λ =1.5405Å) at 60kv and 25mA with scanning speed of 8° in 20 min^{-1} over diffraction angle range.

The micro structure and morphology of the samples were examined by scanning electron microscopy (SEM) using JXA-890 microscope (Jed) at 30 KV.

Differential scanning calorimetry (DSC) was used to determine the changes in the structure, i.e., transition

from one crysatalline form to another, using DSC-50 Shimatzu apparatus. Thermogravimetric analysis (TGA) was performed with a Perkin-Elmer apparatus.

The catalytic hydroconversion processf

All of the catalytic hydroconversion runs were carried out under vapor phase using a fixed-bed down-flow system. The flow system consisted mainly of a vertical tubular silica-glass reactor (1.0 cm internal diameter and 30.0 cm long). Containing 1.0gm of a fresh catalyst, diluted with inert non-porous solid possessing the same dimension of the catalyst particles, was sandwiched between glass wool plugs placed in the middle of the reactor. The reactor was heated in an insulated wider stainless steel tube jacket thermostated to ± 1c°. The temperature of the catalyst bed inside the reactor was measured and controlled via thermocouple and electronic controller, The lower part of the reactor connected to a double condenser attached to a flat flask to collect the liquid products for analysis. Hydrogen gas was used as a carrier and simultaneously as a reactant in the reaction under study, at a flow rate of 20 cm^3 min^{-1} in all runs. Hydrogen was supplied to the system from a cylinder. The liquid feed was pumped to the top of reactor by means of dosing pump. The catalyst was reduced in H_2 at 400°C for 2h. Before starting the reaction runs The reaction was carried out at atmospheric pressure. Toluene and 1,2,4-TMB were passed over the catalyst at $7h^{-1}$ at the requisite ratios and temperatures. The liquid products were collected after an interval of 30 min for analysis using Perkin-Elmer Gas Chromatograph (Model Clarus 500) equipped with capillary column 100m × 0.25ID for PONA analysis (initial temp. 80°c and final temp. 300°c). Detector and injector temperature was 300°c and carrier gas was He with flow rate of 30 ml/min.

RESULTS AND DISCUSSION

TABLE 1 summarizes the characterization results for the H-Y and HD-Y zeolites. The Na content in the H-Y was reduced to 0.11 wt% by ion exchange, and to 0.01 wt% by dealumination. These results indicate that the Na ions were relatively easily exchanged, together with dealumination from the framework. For both H-Y and HD-Y zeolites, the bulk Si/Al ratios were 2.7 and 7, respectively. These results indicate the extraction of Al species during EDTA treatment.

Textural properties

Surface areas, pore volumes and average pore diameters of the prepared supports are listed in TABLE 1. The average pore diameter was calculated by the common definition of 4(pore volume)/surface area. It can be seen that the dealuminated sample represents the lowest surface surface area and highest pore volume. Some mesoporosity created during the chemical dealumination treatments is observed.

FT-IR analysis

The infrared spectra of H-Y and H-DY supports and catalysts in the region of 4000-500cm^{-1} are illustrated in Figure 1. The band at about 1635 cm^{-1} is assigned to a scissor-type vibration band arising from the proton vibration in the water molecules. The bands at 1250 -620 cm^{-1} are assigned to asymetriccal stretching vibrations corresponding to tetrahedral Si,Al atoms[34]

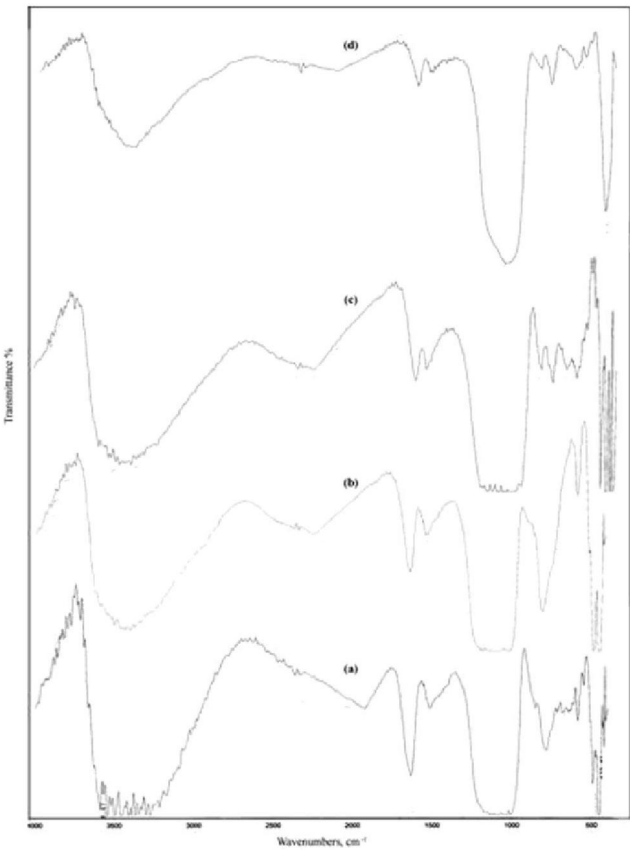

Figure 1 : FT-IR spectra of : (a) H-Y, (b) H-DY, (c) Pt/H-Y, (d) Pt/H-DY

Full Paper

The band between 810 and 700cm^{-1} is assigned to Si-O symmetrical stretching vibration, while the band occurring at 550 to 555cm^{-1} arises from the presence of structural double D6R rings in the case of faujasite zeolite. The band appearing between 465 and 435cm^{-1}can be assigned to the structure - insesitive internal tetrahedral bending bond (T;Si or Al). Careful dealumination of the zeolite with dilute acide opened some of the Si-O-Al bonds and thuse increase in the bulk Si/Al ratio without collapsing the crystalline structure. With dealumination, the intensities of the bands at 730-720 and 620cm^{-1} decreased more significantly. This indicates that aluminum species in the S4R were removed by dealumination. Dealumination also brought about the decrease in the band intensity near 950cm^{-1}, assigned to Si-O stretching vibration[16]. This implies that some hydroxyl nests were formed. Figure (1-b) also shows a large decrease in the peak at 1634cm^{-1}[17].

The IR spectrum in the region of OH stretcting vibration (3800 – 3400cm^{-1}) is also presented in Figure 1. Additional experimental evidence of the formation of hydroxel nest defective sites during the acid pre-treatment step comes from the FT-IR analysis Figure 1. The analysis of the region between 3800-3500cm^{-1} allows for the study of silanol terminal groops[Karge,1998]. In Y zeolite, the O—hH stretch of silanol groups is typically observed at about 3740cm $^{-1}$and the O-H stretch of the strong Bronsted acid site, ie.,Si –o (H)-A,is typically observed at about 3640 cm$^{-1.}$ As one would expect the initial material NH_{4-}Y,after ammonia evacuation in situ at 723k shows a very intense peak at 3640cm due to stronge Bronsted acidity with a negligible peak at 3740hhHH cm^{-1}indicating a low concentration of silanol terminal groups at the external surface of the crystals. The IR spectrum changes significantly after the zeolite was dealuminated. Part of the Bronsted acidity was lost as the presence of silanol terminal group increased, this was shown by a decrease in the the intensity of the peak at 3640cm^{-1}, while the peak at 3740cm^{-1} developed. This is consistent with the extraction of Al from the framework and the consequential formation of hydroxyl nests. Generally,dealumination increases the frequency of IR latt vibration and decreases the intensity of OH –bands (decrease in total acidity). The infrared spectra of Pt/H-Y catalyst and of its dealuminated form are presented in Figure (1c,d). Figure 1-c indicates a shift of the peaks at 684.9 and 589.76cm^{-1} to higher wave numbers at 704.69 and 642.09. Figure 1-d shows a sharp decrease in the intensity of the 799.21 and 588.58cm^{-1} and the appearance of other new peaks at 860.82 and 652.32cm^{-1}. This phenomena shows that Pt exists in more oxide species as PtO_2 and PtO[19], and that Pt particles seems to exist on the outer surface of the two catalysts[20]. The 3640cm^{-1} band which characterize the Bronsted acidity (Figure 1-a) was reduced after Pt loading (Figure 1-c),which means that loading of Pt lowered the Bronsted acidity of H-Y sample[21].

In the OH stretching region 3800-3400cm^{-1}, Figure (1-c) shows a sharp decrease in the intensity of the bands beyond 3640 and 3740cm^{-1} than that of H-DY catalyst (Figure 1-d). The different coverage of the acid OH groups for the two catalysts reflect the shape selectivity as some Pt particles fit into the H-DY channels and other particles present on the outer surface of H-Y catalyst[22]. In other words, the dealumination increases the pore size of H-DY sample. These results are in accordance with the textural properties of the samples (TABLE 1).

The spectra of the two catalysts exhibits a broad band in the range 2150-1920cm constituted by several simple bands are related to different electronic Pt species[23] within the channels, while the spectrum at 2114cm^{-1} is ascribed to the electron deficient platinum at the outer surface[24].

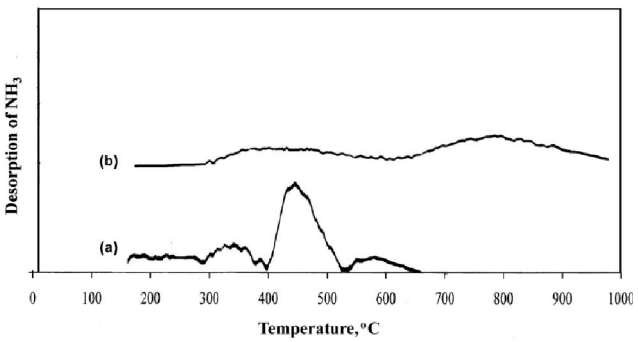

Figure 2 : NH_3-TPD of (a) H-Y and (b) H-DY

The NH_3-TPD spectra of the parent H-Y and H-DY are shown in Figure 2 The peaks resulting from the signal processing have been classified and attributed to three types of acid sites with different acidity strengths, i.e., weak, medium, and strong, according to their position on the chromatogram. The temperature range for

the peak maxima of the weak acid sites has been set between 170 and 190°C, for the medium strength acid sites between 220 and 270°C, and for the strong acid sites above 350°C[25]. H-Y sample showed three main desorption peaks at 350, 450 and 575°C. The H-DY sample shows two main desorption peaks at 425 and 775°C and had a long tailing.

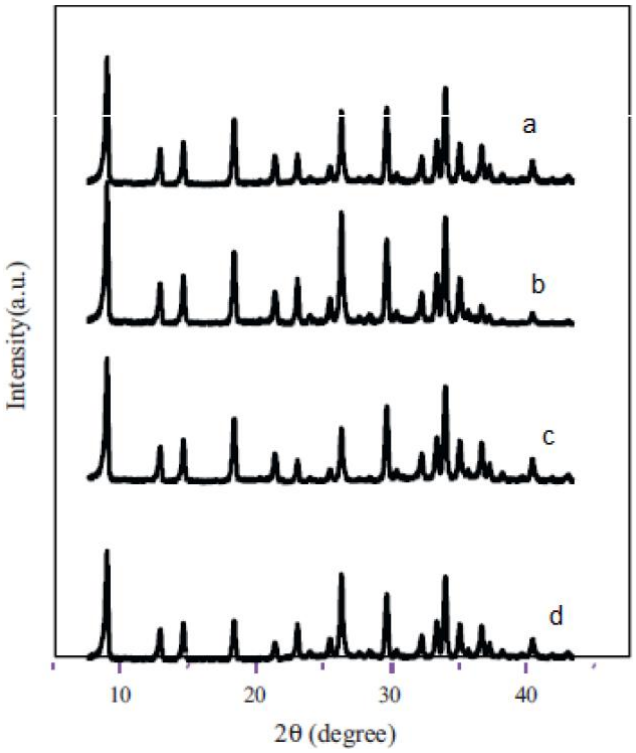

Figure 3 : XRD diffractograms of(a)H-Y,(b)H-DY,(c)Pt/H-Y,(d)Pt//H-DY

XRD analysis was performed to analyze the possible structural changes of the solids after the treatments (dealumination, and impregnation),) to which they were submitted. The XRD patterns of the solids are shown in Figure (3). From the results, the dealuminated sample (H-DY) was well crystallized solid (Figure 3b). Moreover, neither metal impregnation nor dealumination caused significant structural disorder in the samples, considering the fact that their diffractograms were similar to the ones of the parent HYzeolite[11–13]. The Pt modified zeolite samples were not extremely affected by the impregnation process, considering the fact that the cell unity parameter (ao) value of these solids was about 24.3A°, which is similar to that of the parent HY, which had an ao value of 24A°. Indeed, the XRD patterns of the solids do not reflect any Pt phases in the samples (Figuer 3c,d). Thus,it is reasonable that these oxides are on solid surface. However, another possibility is that Pt species are present in low quantities and are undetectable by XRD analysis.

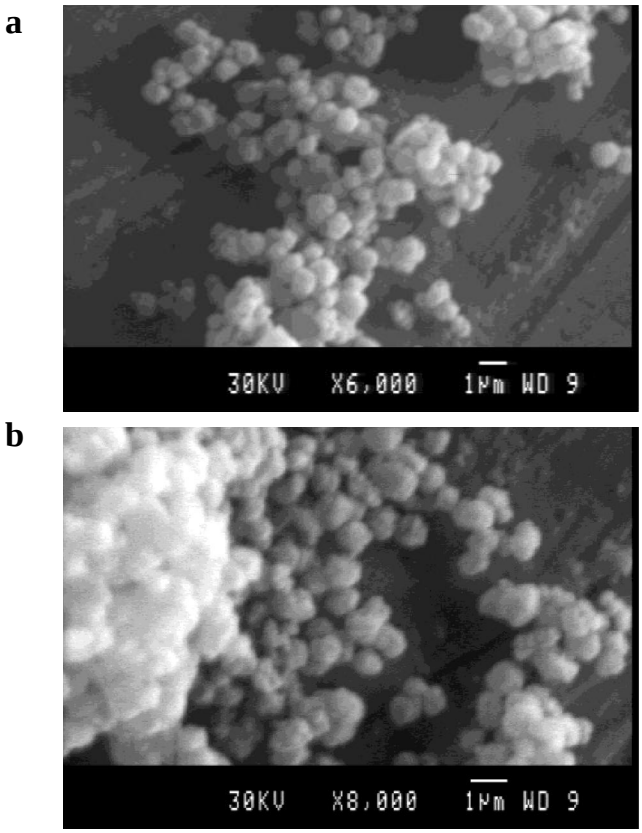

Figure 4 : SEM micrograph of (a) Pt/H-Y, (b) Pt/H-DY

The crystal/particle morphology of the zeolite supports was studied by SEM. In Figure (4) we present the SEM images of representative calcined catalytic material, based on parent NaY zeolite and its dealuminated form. The catalyst based on parent zeolite NaY showed well formed particles/crystallites of cubic-like shape with sharp edges and flat surface with mean size of less than 1 μm. Similar particles/crystallites were observed for the rest of the catalytic materials that were based on dealuminated zeolite; however, as it can be seen in the respective SEM images the dealuminated sample comprised also large aggregates of smaller particles with mean size of 10–40 μm. Formation of these aggregates could happen through binding and consequent condensation of the surface hydroxyl groups (Si–OH) of neighboring crystallites which can be facilitated at the presence of a chemical dealumination agent at relatively lower temperatures in aqueous media which generates a high number of hydroxyl nests

Full Paper

when aluminum atoms are removed from the framework[35].

The DSC/TGA of calcined, reduced and used samples are shown in Figure 5. All of these samples show two main endothermic effects. The first endothermic peaks located at 136.7 and 156.6°C (Figure 5 a, b) are related to the loss of water. Due to the microporous structure of Pt/H-Y, water is librated at higher temperature than the dealuminated sample. However, following the dehydration period, the endotherm observed at 442 – 460°C is due to decomposition of oxide precursor.

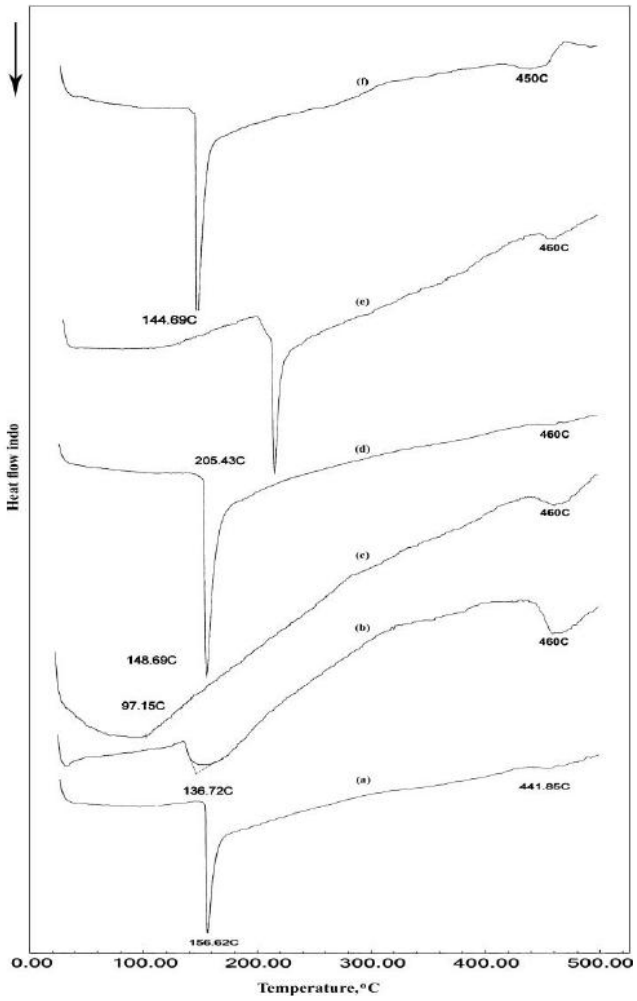

Figure 5 : DSC profiles of: (a) Pt/H-Y, (b) Pt/H-DY, (c) Pt/H-Y reduced, (d) Pt/H-DY reduced, (e) Pt/H-Y used, (f) Pt/H-DY used

The reduced catalysts show endothermic peaks at 97 and 148.69°C which are attributed to the libration of water with the formation of metal oxide phases (Figure 5 c, d). The endothermic peak at 460°C is ascribed to change from reduced state to oxide state.

The endothermic pattern at 205.4°C (Figure 5-e) of the used Pt/H-Y catalyst is attributed to the decomposition of highly volatile species and light coke precursors[7]. Also, the sharp endothermic pattern in the region of water; 144.69°C are due to oxidation of the metallic phase (Figure 5-f). The endothermic peaks at 450 - 460°C due to phases change. TABLE 2 shows the losses of weight as the increase of temperature as obtained from thermogravimetric analsysis (TGA).

TABLE 2 : The results of thermogravimetric analysis

Catalyst	Pt/H-Y			Pt/H-DY		
	Calcined	Reduced	Used	Calcined	Reduced	Used
Endothermic temp., °C	156.6	97.15	205.43	136.72	148.69	144.7
Weight loss, %	1.62	2.52	3.1	1.38	1.72	2.2
Endothermic temp., °C	442	460	460	460	460	450
Weight loss, %	1.56	2.4	3	1.33	1.69	2.0

Catalyst performance test

During the process of toluene transalkylation by trimethyl benzene, besides the transalkylation reaction (1), a series of secondary reactions take place. Evidently, the following transformation can be considered: disproportionation of toluene (2) and trimethyl benznes (2‘), respectively, and the isomerization of xylenes (3), resulted from transalkylation and the two disproportionation reactions, and the isomerization of trimethyl benzene (3‘) used as the starting reactant (Scheme 1).

(1) $T + TMB \Rightarrow 2X$

(2) $2T \Rightarrow B + X$

(2`) $2TMB \Rightarrow X + TeMB$

(3) $pX \Rightarrow mX \Rightarrow oX$

(3`) $1,2,4-TMB \Rightarrow 1,3,5-TMB \Rightarrow 1,2,3-TMB$

The conversions, either by disproportionation or transalkylation, of toluene (X_T), and trimethylbenzene (X_{TMB}) are defined as:

$$X_T = \frac{(\text{toluene wt\%})_F - (\text{toluene wt\%})_P}{(\text{toluene wt\%})_F}$$

$$X_{TMB} = \frac{(\text{TMB wt\%})_F - (\text{TMB wt\%})_P}{(\text{TMB wt\%})_P}$$

Since 1,2,4-TMB can simultaneously undergo reactions of isomerization and disproportionation, we define the

overall apparent selectivity of these reactions as:

$$S_I(\text{mol/mol}) = \frac{(1,3,5-\text{TMB wt\%})_P + (1,2,3-\text{TMB wt\%})_P}{100-(1,2,4-\text{TMB wt\%})_P}$$

$$S_D(\text{mol/mol}) = \frac{2(\text{TeMB wt\%})_P/134}{\left[100-(1,2,4-\text{TMB wt\%})_P\right]/120}$$

$$\frac{S_D}{S_I}(\text{mol/mol}) = \frac{2(\text{TeMBwt\%})_p/134}{\left[(1,2,4-\text{TMBwt\%})p+((1,2,4-\text{TMBwt\%})p)\right]/120}$$

Where, the subscripts F and P represent the composition of components in the feed stream and in the product stream, respectively. S_I is selectivity of isomerization and S_D is selectivity of disproportionation[22].

Influence of reaction temperature

The reaction between 1,2,4-TMB and toluene has been investigated using Pt/H-Y catalyst. Experiments were performed to select the optimum reaction temperature suitable to study the correlation between feed composition and conversion. Also to compare the mentioned catalyst with the dealuminated catalyst (Pt/H-DY). Figure 6 shows that the yield of xylenes in the conversion product increases rapidly from 300 to 350°C, then a slight increase is observed leading to a maximum yield of xylene isomers at 400°C. These temperatures will be adopted in all the reaction experiments.

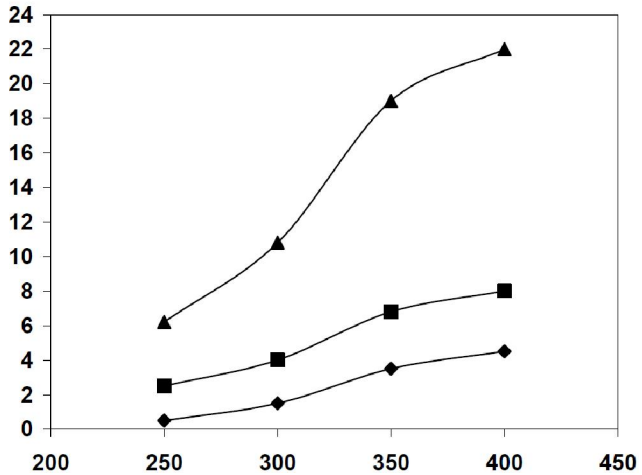

Figure 6 : Product yields as a function of reaction temperature in transalkylation of 1,2,4-TMB and toluene: (♦) xylenes; (■) 1,3,5-TMB+1,2,3-TMB; (▲) TeMB. (LHSV, 7h^{-1}, H_2 flow rate: 20ml/min, $\frac{1,2,4-\text{TMB}}{T}=1/1$)

Tetramethylbenzenes (TeMB) yields increase slightly with the increase in reaction temperature; it was associated (attributed) with a slow diffusivity of TeMBs, which were probably accumulated in the channel system of zeolite in a similar way as described for m-xylene in ZSM-5[26]. This led to significant changes in the concentration of aromatics in the zeolite channels and it is assumed that the methyl transfer between adsorbed TMBs and TeMB proceeded in a large extent Figure 6. Another remark consists in the fact that the total conversion of TMB is higher than the total conversion of toluene for all temperatures Figure 7.

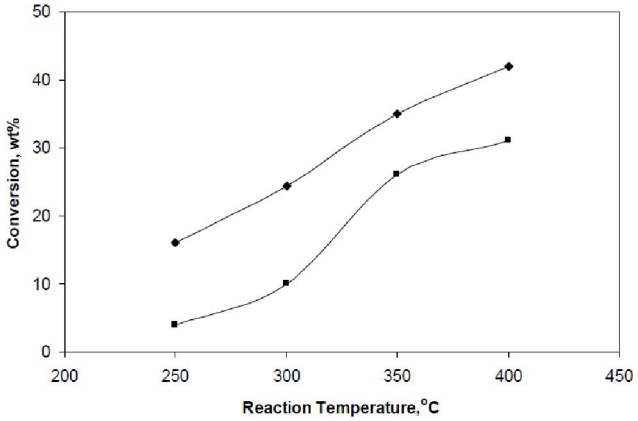

Figure 7 : Conversion of 1,2,4-TMB and toluene as a function of reaction temperature: (♦) 1,2,4-TMB, (■) toluene (LHSV, 7h^{-1}, H_2 flow rate: 20ml/min, $\frac{1,2,4-\text{TMB}}{T}=1/1$)

TMB isomerization proceeds by the similar carbocationic mechanism as proposed by Corma and coworkers[27] for xylene isomerization. It includes adsorption of one TMB molecule and formation of protonated TMB cation, which further reacts with another TMB molecule strongly held by the electrostatic field in the zeolite channel.

Referring to the distribution of xylene isomers, this is close to those of thermodynamic equilibrium (1,2,4-TMB → mX and o-X) once the xylenes are formed, they tend to isomerize towards the thermodynamic composition Figure (8-a). Similar results have been obtained by dumitriu et al.[28].

Figure (8-b) shows that in isomerization, 1,2,4-TMB gives more 1,3,5-TMB than 1,2,3-TMB. Among the two isomers, the molecular size of 1,3,5-TMB is the largest[28]. Therefore, 1,2,3-TMB has a diffusion advantage over the 1,3,5-isomer. If the shape selectivity of the TMB isomers comes into effect, selectivity of the 1,2,3-isomer formation should be greater than selectivity of the 1,3,5-isomer. Nevertheless, the 1,3,5-

isomer is the thermodynamically favorable over the 1,2,3-isomer[29].

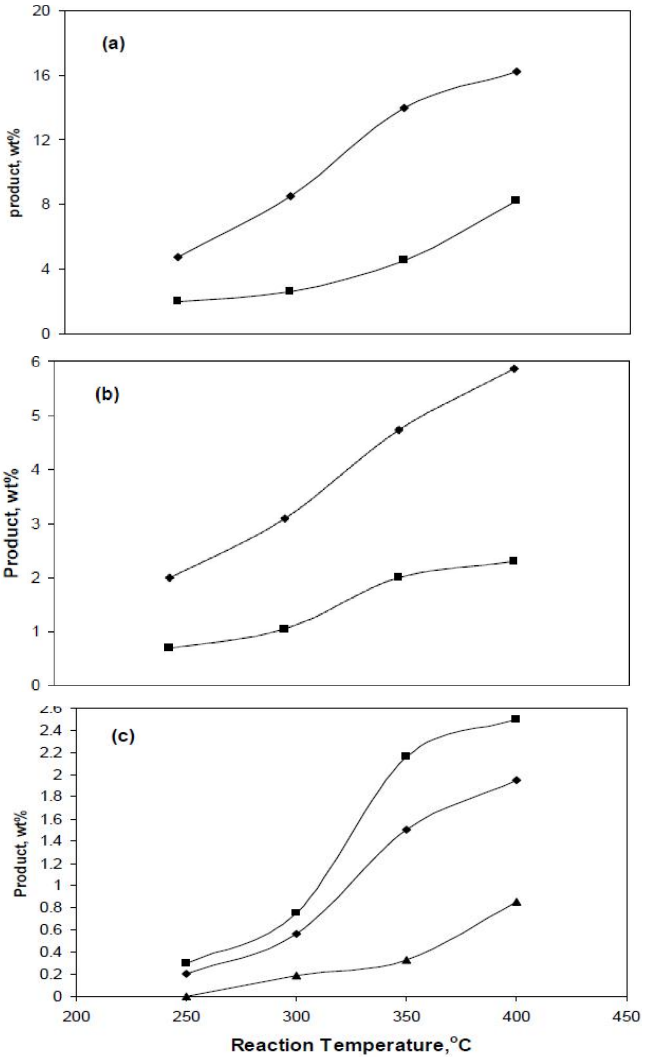

Figure 8 : Product distribution as a function of reaction temperature; (a) ♦ m-X+p-X; ■. o-X, (b) ♦ 1,3,5-TMB; ■ 1,2,3-TMB, (c) ■1,2,3,5-TeMB; ♦ 1,2,4,5-TeMB; ▲ 1,2,3,4-teMB (LHSV, 7h^{-1}, H_2 flow rate: 20ml/min)

The isomer distribution of the TeMB is a shape-selective reaction and is an explanation to the thermodynamic equilibrium[30] (Figure 8-c). At high reaction temperatures, TMB preferentially undergoes disproportionation to isomerization Figure (9).

Assuming that xylene is produced only by transalkylation, the xylene production efficiency (on a molar basis) of TMB (E_{TMB}) and of toluene (E_T) can be calculated as:

$$E_{TMB} = \frac{0.5(\text{xylene wt\%})/106}{\left[(1,2,4-\text{TMB wt\%})_F - (1,2,4-\text{TMB wt\%})_P\right]/120}$$

$$E_T = \frac{0.5(\text{xylene wt\%})/106}{\left[(\text{toluene wt\%})_F - (\text{toluene wt\%})_P\right]/92}$$

Their levels of efficiency are plotted in Figure (10)versus the reaction temperature. Evidently, at 300°C the efficiency of toluene is much greater than that of TMB and at 250°C TMB shows a substantial conversion. Therefore, it is reasonable to believe that transalkylation is initiated by TMB, where the TMB molecules are first adsorbed on active sites inside the zeolite pores. The adsorbed TMB molecules then form carbonium ions, which are ready form monomolecular isomerization, bimolecular disproportionation with another TMB molecules, or transalkylation with toluene molecules. The diffusivity of TMB is lower than that of toluene; therefore, the toluene concentration inside the zeolite pores should be much higher than the TMB concentration. Then, the adsorbed TMB carbonium ions will have a higher possibility of reacting with toluene molecules rather than with TMB molecules. Thus, a methyl group is transferred from TMB carbonium ion to one toluene molecule and form 2 mol of xylenes. Toluene then plays a role as a scavenger, removing methyl group from TMB, and becomes the controlling species of transalkylation[31]. In contrast, at high reaction temperature, TMB preferentially undergoes disproportionation to isomerization Figure 9 and the xylene production efficiency of TMB is raised accordingly. On the basis of the above discussion, it is clearly revealed that the methyl group is exclusively transferred from TMB to toluene. The result of the reactions showed a few percent of light gases (24w%) at 400C and total C_7- C_9 saturates (54w%) at the same temperature.

The effect of feed composition

Reaction results of 1,2,4-TMB and toluene at various TMB-to toluene ratio (TMB/T) are shown in TABLE 3. With the increase of TMB to toluene in the feed, both xylenes formation and TMB conversion increase continuously which indicates that disproportionation of TMB becomes the dominant reaction at higher TMB contents in the feed. Also the higher concentration of TMB relative to that of toluene in the pore of zeolites would enhance the transfer of a methyl group from TMB molecule to another TMB molecule with the formation of TeMB. Benzene yield, which is a good

indication of toluene disproportionation, is substaintially reduced in accordance with the increase TMB/toluene ratio, which may indicate that it is almost not formed or a side reaction between benzene and TMB proceeds very rapidly towards xylene production. The results presented in column 3 at low ratio of TMB/toluene indicate that TMB is much more reactive than toluene. Comparing the last two columns in TABLE 3, the yield of TeMB and the disproportionation selectivity of TMB is lowered by adding 50% of toluene into the TMB feed; there are also some decrease of TMB conversion. Obviously, the presence of both reagents in the feed leads to a significant dilution of the alkylaromatics (TMB, toluene) and, subsequently, the transalkylation reaction is favored.

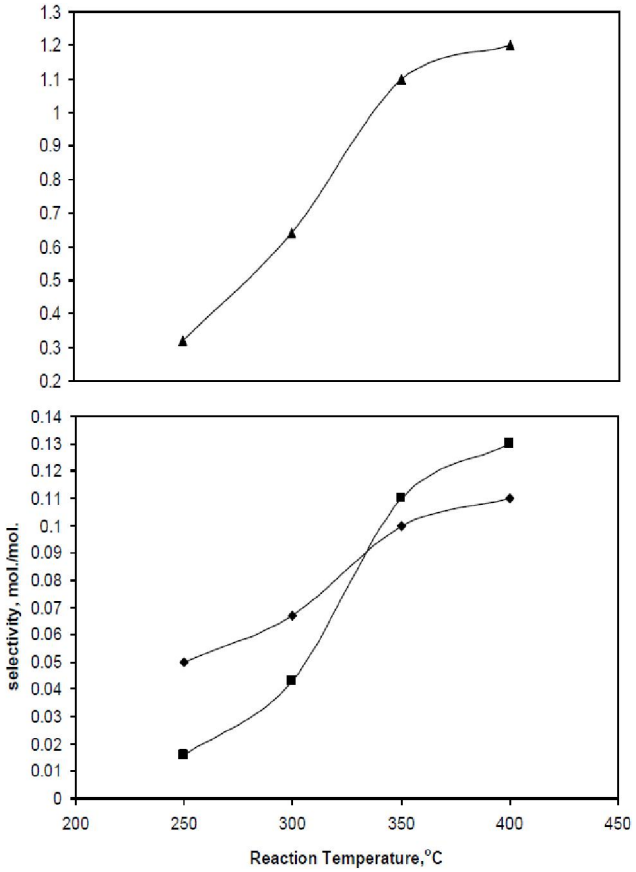

Figure 9 : Selectivities as a function of reaction temperature: (♦) S_I; (■) S_D; (▲) S_D/S_I (LHSV, 7h^{-1}, H_2 flow rate: 20ml/min, $\frac{1,2,4-TMB}{T} = 1/1$)

The competition between the disproportionation and the transalkylation reactions can also be explained on the basis of the reaction mechanism. The two reactions occur via a bimolecular mechanism with a diphenylmethane intermediate[29]. Under these conditions the disproportionation reaction requires the presence of two identical molecules on two neighboring sites; but this requirement is not fully satisfied due to the presence of the second reagent which will favor the transalkylation reaction.

TABLE 3 : Product distribution from the conversion of 1,2,4-TMB and toluene over Pt/H-Y and Pt/H-DY catalysts (reaction temperature: 400°C, LHSV: 7h^{-1} and H_2 flow rate = 20 ml/min)

Catalyst	Pt / H-Y			Pt / H-DY	
Feed composition, wt%.					
1,2,4-TMB	67.3	50	32.7	50	100
Toluene	32.7	50	67.3	50	0.0
1,2,4-TMB/toluene	2/1	1/1	1/2	1/1	-
Product distribution, wt%					
Light gases	0.3	0.24	0.0	0.85	1.8
C_7 – Saturates	0.01	0.27	0.0	0.29	0.35
C_8 – Saturates	0.08	0.17	0.04	0.23	0.33
C_9 – Saturates	0.04	0.10	0.0	0.17	0.22
Benzene	0.10	0.20	0.34	0.24	0.10
Toluene	16.9	34.5	51.56	34.0	3.5
Xylene	28.5	22	18	27	20.11
p-X + m-X	21.5	16.8	13.7	20.0	15.11
o-X	7	5.2	4.3	7.0	5.0
TMBs					
1,3,5 - TMB	10	5.86	4.5	4	10.2
1,2,4 - TMB	31	29	21.2	23.0	35.87
1,2,3 - TMB	3.5	2.3	1.5	2.0	3.5
TeMBs	9.5	5.3	2.8	8.02	24.0
1,2,4,5 - TeMB	3.5	1.95	0.9	3.0	9
1,2,3,5 - TeMB	4.8	2.5	1.5	4.0	12
1,2,3,4 - TeMB	1.2	0.85	0.4	1.02	3
Otheres	Traces	Traces	Traces	Traces	Traces
Conversion, wt%					
1,2,4 - TMB	53.9	42	35.17	50.14	64.13
Toluene	48.3	31	23.4	32	-
Reaction selectivity, wt/wt					
S_I, mol/mol	0.2	0.11	0.08	0.10	0.21
S_D, mol/mol	0.26	0.13	0.06	0.14	0.70
S_D/S_I, mol/mol	1.3	1.2	0.75	1.4	3.33

S_I: Selectivity of isomerization., S_D: Selectivity of disproportionation

H-DY showed higher catalytic activity than H-Y in spite of the decrease in total acid sites content. Ac-

Full Paper

cording to infrared spectra (Figure 1), H-DY has more open structure and thus the acid sites become exposed to the main channel, and these acid sites can serve as new adsorption sites for toluene and TMB. In addition, the more open structure of H-DY would facilitate the diffusion of TMB; this is supported by the results given in TABLE 3 (column 2 and 4) where the toluene conversion is only slightly increased over H-DY whereas the conversion of 1,2,4-TMB, is considerably increased from 42% for H-Y to 50.14 for H-DY (column 4 of TABLE 3). This means that the higher yield of xylene isomers over H-DY is mainly attributed to the increase of reactivity of 1,2,4-TMB. The two features described above are understood to compensate for the loss of total acid sties, and give rise to the high activity[31].

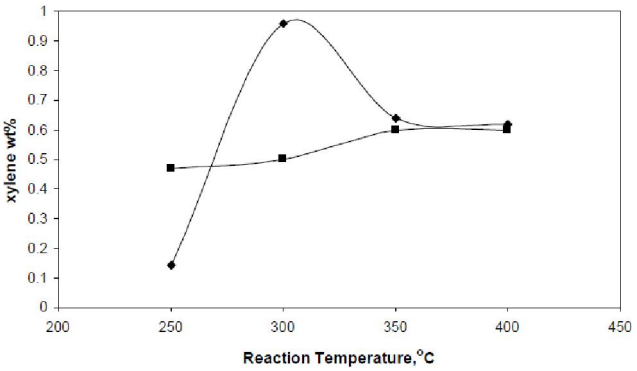

Figure 10 : Plot of theoritical xylene production efficiency of toluene and 1,2,4-TMB as a function of reacton temperature: (♦) E_T; (■) E_{TMB} (LHSV, 7h^{-1}, H_2 flow rate: 20ml/min, $\frac{1,2,4-TMB}{T} = 1/1$)

The results discussed above show that among the H-Y zeolite, dealuminated catalyst showed high activity and stability (Figure 11) for transalkylation reaction. In conclusion Pt/H-Y could be a potential acid catalyst for transalkylation of 1,2,4-TMB and toluene if the parent zeolite is subjected to precautious dealumination by EDTA.

The stability of the catalysts

The degree of 1,2,4-TMB conversion over the two catalysts was compared at two reaction temperatures (250°C and 400°C). Figure 11 shows 1,2,4-TMB conversions versus time on stream (T-O-S). For the two catalysts, highest conversion of 1,2,4-TMB was measured over the dealuminated catalyst at the reaction conditions used. An interesting effect in the catalytic behavior of the low Si/Al material (Pt/H-Y) was observed at the lower reaction temperature (250°C). Compared to the dealuminated catalyst, the low Si/Al sample having the highest concentration of bridging hydroxyls of the weakest acidity seemed to possess fast deactivation. It has been reported that coke is formed preferentially on the catalyst with high acid density than on catalyst with low acid density where coke percentage on H-Y and H-DY catalysts are 1,1 and 0.7 wt%, respectively. Evidently, it is the combination of the zeolite pore structure and its acidity (controlled by dealumination) that can result in time stable activity[32].

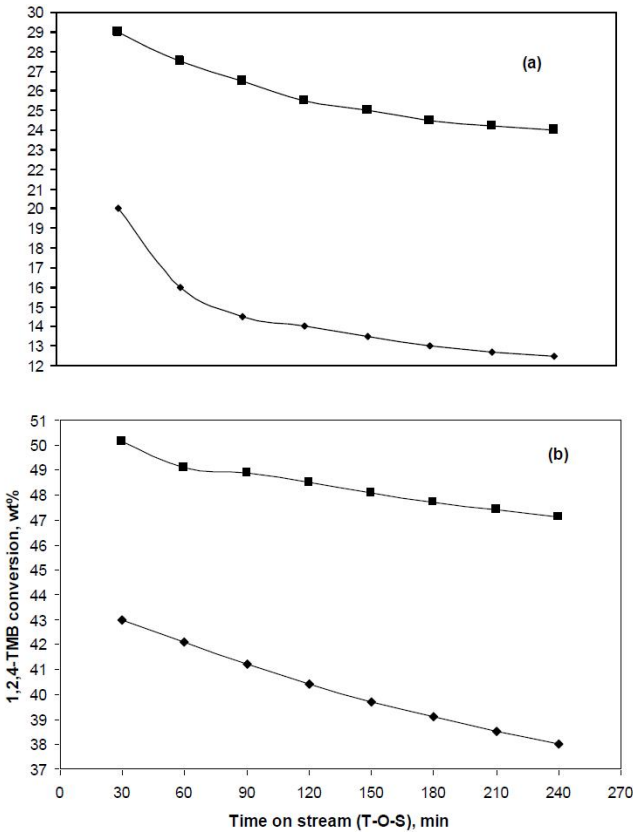

Figure 11 : 1,2,4-TMB conversion as a fucntion of time on stream at: (a) 250°C, (b) 400°C: (■) Pt/H-DY, (♦) Pt/H-Y

CONCLUSIONS

A good correlation has been found between the Brönsted acidity characteristics (number and strength of the acid sites) and the catalytic performance of the parent H-Y and the dealuminated H-DY supported catalysts.

The activity sequence passes through a maximum for the Pt/H-DY catalyst.

The Pt/H-Y catalyst, with greater amounts of weak acid sites, shows the higher percent of coke; this is most probably due to the strongly accelerated processes of adsorption and accumulation of the reactant and the products especially at lower reaction temperatures. The lowest activity of Pt/H-Y catalyst is mainly attributed to diffusion limitations and product inhibition.

The correlation of the acidity measurements and catalytic tests indicates that the transalkylation and disproportionation reactions occur on medium and strongly acid sites, while the isomerization reaction is activated even on weak acid sites.

It is noted that for the aromatics conversion system studied here, the reactant feeds as well as the xylene products are likely to be hydrogenated. As the consequence of hydrogenation reactions, the formation of saturates may also deteriorate the purity of aromatic products. In this context the preparation of an ideal metal catalyst for transalkylation process that resulted in minimum yield of saturates while maintaining good catalytic stability remains a challenging task.

REFERENCES

[1] M.M.Jorge, F.F.Gilbert; Alkylation on solid acids, Part 2, single – even kinetic modeling. Ind.Eng. Chem.Res., **45**, 954-967 **(2006)**.

[2] J.M.Martinis, G.F.Froment; Solid acid alkylation, Part-1, Experimental investigation of catalytic deactivation. Ind.Eng.Chem.Res., **45**, 940-953 **(2006)**.

[3] S.Al-Khattafa, M.N.Akhtara, T.Odedairoa, A.Aitani, N.M.Tukur, M.Kubu, Z.Musilova-Pavlaˇckovab, J.Cejkab; Appl.Catal., **A394**, 176-190 **(2011)**.

[4] B.H.Anand; Shape selective alkylation over pore engineered zeolite catalysts – IPCL's approach from concept to commercialization. Bull.of Catal.Soc.of India, **2**, 184-193 **(2003)**.

[5] R.Bandyopadhyay, Y.Sgi, Y.Kubota, R.S.Rao; Trnasalkylation reaction–an alternative route to produce industrially important intermediates such as cymene. Catal.Today, **44**, 245-252 **(1998)**.

[6] K.Tanab, W.F.Holderich; Industrial application of solid acid-base catalysts. Appl.Catal.A, **181**, 399 **(1999)**.

[7] V.Mavrodinova, M.Popova, R.M.Mihalyi, G.Pal-Borbely, C.Minchev; Transalkylation of toluene with cumene over zeolites Y dealuminated in solid-state, Part II, Effect of the introduced lewis acid sties. Appl.Catal.A, **248**, 197-209 **(2003)**.

[8] M.-A.Heiddy, A.D.Silva, H.G.S.Priscilla, M.C.Alex, H.-V.Ricardo, A.G.A.Donato, O.A.C.Antunes; Transalkylation of polyalkylbenzenes catalyzed by lewis acids. Catal.Communications, **5**, 221-224 **(2004)**.

[9] I.Wang, T.-C.Isai, S.-T.Huang; Disproportionation of toluene and of trimethylbenzene and their transalkylation over zeolite Beta. Ind.Eng.Chem. Res., **29**, 2005-2012 **(1990)**.

[10] G.T.Kerr; Chemistry of crystalline aluminosilicates, VI, Preparation and properties of ultrastable hydrogen zeolite Y. J.Phys.Chem., **72**, 1385-1390 **(1968)**.

[11] V.Mavrodinova, M.Popova, G.Pal Borbely, R.M.Mihalyi, C.Minchev; Transalkylation of toluene with cumene amit over zeolites Y dealuminated in solide – state, Part I, Effect of the alteration of Bronsted acidity. Appl.Catal.A, **248**, 181-196 **(2003)**.

[12] K.A.-G.Ahmed, M.A.-F.Sameh, A.K.A.-G.Noha; Hydroconversion of cyclohexene using catalysts containing, Pt, Pd, Ir and Re supported on H-ZSM-5 zeolite. Appl.Catal.A., **283**, 157-164 **(2005)**.

[13] F.Bauer, W.-H.Chen, H.Ernst, S-J.Huang, A.Freyer, S.-B.Liu; Selectivity improvement in xylene isomerization. Micro.and Meso.Materials, **72**, 81-89 **(2004)**.

[14] S.Barman, S.K.Maity, C.Pradhan; Alkylation of toluene with isopropyl alcohol catalyzed by ce-exchanged NaX zeolite. Chemical Eng.J., **114**, 39 **(2005)**.

[15] G.Coudurier, C.Naccache, J.C.Vedrine; Users of i.r-spectrospcopy in identifying ZSM zeolite structure. J.Chem.Soc.Chem.Commun., 1413 **(1982)**.

[16] P.C.Van Geem, K.F.M.G.J.Scholle, G.P.M.Van der Veid; Study of the transformation of small-port into large-port mordenite by magic-angle spinning NMR and IR spectroscopy. J.Phys.Chem., **92**, 1585 **(1988)**.

[17] S.M.Babitz, M.A.Kuehene, H.H.Kung, J.T.Miller; Role of Lewis acidity in the deactivation of USY zeolites during 2-methylpentane cracking. Ind.Eng.Chem.Res., **36**, 3027-3031 **(1997)**.

[18] C.Morterra, C.Emanual, G.Cerrato, G.Magnacca; J.Chem.Soc.Faraday Trans., **88**, 339 **(1992)**.

[19] A.V.Ivanov, T.V.Vasina, O.V.Masloboishchikova, E.G.Khelkovskaya Sergeva, L.M.Kustov,

J.F.Houzvicka; Isomerization of n-alkanes of Pt/WO_3-SO_4/ZrO_2 systems. Catal.Today, **73**, 95-103 **(2002)**.

[20] J.Oi-Uchisawa, S.Wang, T.Nanba, A.Ohi, A.Obuchi; Improvement of Pt catalyst for soot oxidation using mixed oxide as a support. Appl.Catal.B., **44**, 207-215 **(2003)**.

[21] J.-L.Dong, T.-H.Zhu, Q.-H.Xu; Influence of structure and acidity-basicity of zeolites on platinum supported catalysts of n-C_6 aromatization. Appl.Catal.A, **112**, 105-115 **(1994)**.

[22] C.Jiri, K.Josef, K.Andrea; Disproportionation of trimethylbenzenes over large pore zeolites: Catalytic and adsorption study. Appl.Catal.A., **277**, 191-199 **(2004)**.

[23] A.Adolfo, L.S.Xosé, G.Javier; Surface characterization and dehydrocyclization activity of Pt/KL catalysts prepared by different methods. Appl.Surface Science, **205**, 206-211 **(2003)**.

[24] J.M.Graw, L.Daza, X.L.Seoane, A.Arcoya; Effect of Ba and rare earths cations on the properties and dehydrocyclization activity of Pt/k-LTL catalysts. Catal.Lett., **53**, 161-166 **(1998)**.

[25] E.Dumitriu, V.Hulea, S.Kaliaguine, M.M.Huang; Transalkylation of the alkylaromatic hydrocarbons in the presence of ultrastable Y zeolites. Transalkylation of toluene with trimethylbenzenes. Appl.Catal.A, **135**, 57-81 **(1996)**.

[26] G.Mirth, J.Cejka, J.A.Lercher; Transport and isomerization of xylenes over HZSM-5 zeolites. J.Catal., **139**, 24-33 **(1993)**.

[27] A.Corma, F.Llopis, J.B.Monton; Influence of the structural parameters of Y zeolite on the transalkylation of alkylaromatics. J.Catal., **140**, 384 **(1993)**.

[28] E.Dumitriu, C.Guimon, V.Hulea, D.Lutic, I.Fechete; Transalkylation of toluene with trimethylbenzenes catalyzed by various AFI catalysts. Appl.Catal.A, **237**, 211-221 **(2002)**.

[29] M.Kojima, R.Hartford, C.T.O'connor; The effects of pillaring montmorillonite and beidellite on the conversion of trimethylbenzenes. J.Catal., **128**, 487 **(1991)**.

[30] H.W.Earhart; Polymethylbenzene. Kirk-Othmer Encyclopedia of chemical technology, Wiley: New York, **18**, 882 **(1982)**.

[31] K.J.Chao, L.J.Leu; Conversion of toluene and trimethylbenzene over NaH Y zeolites. Zeolites, **9**, 193-196 **(1989)**.

[32] S.Al-Khattaf, A.Lliyas, A.Al-Amer, T.Inui; The effect of Y-zeolite acidity on m-xylene transformation reactions. J.Molecular Catal.A: Chemical, **225**, 117-124 **(2005)**.

[33] H.G.Karge; Microporous Mater., **22**, 495-666 **(1998)**.

[34] P.Morales-Pachecoa, J.M.Domínguezb, L.Bucioa, F.Alvarezb, U.Sedranc, M.Falcoc, Synthesis of FAU(Y)- and MFI(ZSM5)-nanosized crystallites for catalytic crackingof 1,3,5-triisopropylbenzene. Catalysis Today, **166**, 25-38 **(2011)**.

[35] K.S.Triantafyllidis, S.A.Karakoulia, D.Gournis, A.Delimitis, L.Nalbandian, E.Maccallini, P.Rudolf; Formation of carbon nanotubes on iron/cobalt oxides supported on zeolite-Y: Effect of zeolite textural properties and particle morphology. Microporous and Mesoporous Materials, **110**, 128-140 **(2008)**.